Biomaterials and Biosystems 8 (2022) 100069

Contents lists available at ScienceDirect

Biomaterials and Biosystems

journal homepage: www.elsevier.com/locate/bbiosy

Antimicrobial-free graphene nanocoating decreases fungal yeast-to-hyphal switching and maturation of cross-kingdom biofilms containing clinical and antibiotic-resistant bacteria

Shruti Vidhawan Agarwalla[a], Kassapa Ellepola[b], Vitaly Sorokin[c,d], Mario Ihsan[c], Nikolaos Silikas[e], AH Castro Neto[f], Chaminda Jayampath Seneviratne[g,**], Vinicius Rosa[a,f,h,*]

[a] Faculty of Dentistry, National University of Singapore, Singapore
[b] Department of Oral Biology, College of Dentistry, University of Illinois Chicago, USA
[c] Department of Surgery, Yong Loo Lin School of Medicine, National University of Singapore, Singapore
[d] Department of Cardiac, Thoracic and Vascular Surgery, National University Hospital, National University Health System, Singapore
[e] Dentistry, The University of Manchester, Manchester, United Kingdom
[f] Centre for Advanced 2D Materials, National University of Singapore, Singapore
[g] School of Dentistry, The University of Queensland, Australia
[h] ORCHIDS: Oral Care Health Innovations and Designs Singapore, National University of Singapore, Singapore

ARTICLE INFO

Keywords:
Implant
Nanomaterial
Titanium
Mixed-microbial infection
Peri-implantitis
Integration
Anti-adhesive surface modification
Biofouling

ABSTRACT

Candida albicans and methicillin-resistant *Staphylococcus aureus* (*MRSA*) synergize in cross-kingdom biofilms to increase the risk of mortality and morbidity due to high resistance to immune and antimicrobial defenses. Biomedical devices and implants made with titanium are vulnerable to infections that may demand their surgical removal from the infected sites. Graphene nanocoating (GN) has promising anti-adhesive properties against *C. albicans*. Thus, we hypothesized that GN could prevent fungal yeast-to-hyphal switching and the development of cross-kingdom biofilms. Herein, titanium (Control) was coated with high-quality GN (coverage > 99%). Thereafter, mixed-species biofilms (*C. albicans* combined with *S. aureus* or *MRSA*) were allowed to develop on GN and Control. There were significant reductions in the number of viable cells, metabolic activity, and biofilm biomass on GN compared with the Control (CFU counting, XTT reduction, and crystal violet assays). Also, biofilms on GN were sparse and fragmented, whereas the Control presented several bacterial cells co-aggregating with intertwined hyphal elements (confocal and scanning electronic microscopy). Finally, GN did not induce hemolysis, an essential characteristic for blood-contacting biomaterials and devices. Thus, GN significantly inhibited the formation and maturation of deadly cross-kingdom biofilms, which can be advantageous to avoid infection and surgical removal of infected devices.

1. Introduction

Titanium and its alloys have excellent biocompatibility and promising physical, mechanical, and good corrosion resistance, hence being widely used in the fabrication of catheters, pacemakers, dental and orthopaedic implants [1,2]. Nonetheless, titanium alloys are vulnerable to microbial infection triggering inflammation and tissue destruction. These can lead to clinical failure and demand surgical removal of the implant or device from the infected site [3,4]. Removing infected devices from less accessible sites (like pacemakers and orthopaedic implants) or from health compromised patients, might be challenging, costly or even life-threatening [4].

Some of the most concerning biofilms are formed by polymicrobial conglomerates where the pathogenssynergize, and present amplified virulence [5]. Polymicrobial infections have been associated with higher mortality rates (70%) when equated to a single-species microorganism infection (23%) [6]. *Candida albicans* and *Staphylococcus aureus* are co-infector microorganisms on biomedical implants [7]. *C. albicans* is the most frequently occurring opportunistic pathogenic fungus, able to form biofilms that are directly associated with therapeutic failure and mortality [8,9]. Candida-related infections in vascular catheters have

* Corresponding author at: Faculty of Dentistry, National University of Singapore, 9 Lower Kent Ridge Road, 119085, Singapore.
** Co-corresponding author at: School of Dentistry, The University of Queensland, 288 Herston Road, Cnr Bramston Terrace & Herston Road Herston QLD 4006, Australia.
E-mail addresses: jaya.seneviratne@uq.edu.au (C.J. Seneviratne), vini@nus.edu.sg (V. Rosa).

https://doi.org/10.1016/j.bbiosy.2022.100069
Received 5 April 2022; Received in revised form 23 October 2022; Accepted 23 October 2022

high mortality rate [10]. *S. aureus* is an opportunistic pathogenic bacterium identified as one of the leading causes of nosocomial and indwelling device–associated infections [11]. Its methicillin-resistant version (*MRSA*) has high virulence and it has been associated with augmented morbidity, low rates of overall cure (57%), and post-infection sequelae in total joint arthroplasty infections and other orthopaedic implant infections [12,13]. Cross-kingdom biofilms formed by *C. albicans* and *S. aureus* has high virulence and resistance to immune defense and antimicrobial agents [7]. Notably, *in vivo* studies have shown that *C. albicans* and *S. aureus* synergize to increase mortality and morbidity [14,15]. *C. albicans* and *S. aureus* have been co-isolated on infected central venous catheters and patients suffering from denture stomatitis [16,17].

Biomedical implants and devices made of titanium do not have inherent antimicrobial properties and non-surgical treatments are the preferred choice to subdue implant infections. Mechanical debridement and detoxification with antiseptics are often used in conjunction to treat infected dental implants. However, this therapy may not be able to re-establish fully tissue health and bone integration [18,19]. Contrary to diseased dental implants whose infected portion may be accessed for detoxification, internal medical devices (*e.g.*, long-term hemodialysis catheters or pacemakers) are out of reach for mechanical debridement, or may be in contact with tissues that may not tolerate chemical cleaning Contrary to diseased dental implants. In these cases, clinicians opt for antimicrobial therapies which may have limited efficacy against polymicrobial biofilm infections. For instance, *S. aureus* exhibits increased antibiotic resistance against vancomycin in the presence of *C. albicans* [20]. Likewise, *C. albicans* presents higher tolerance toward fluconazole and miconazole in the presence of *S. epidermidis* and *S. aureus* [21,22].

Treating cross-kingdom infections is very challenging since the therapeutics frequently target pathogens within each kingdom, and due to the risks associated with the rise of antibiotic-resistant bacteria [23,24]. Hence, strategies that prevent polymicrobial biofilm formation or its maturation are of high interest. In this context, graphene nanocoating (GN), a cytocompatible platform [25–30] that can be deposited on dental and orthopaedic implants, renders promising anti-adhesive properties against fungi, gram-positive and -negative bacteria [31,32]. Notably, GN hampers the adhesion of unicellular *C. albicans* to titanium, deterring biofilm growth and maturation, and the transition from yeast to hyphae form, for up to seven days [33]. Since the hyphae harbors *S. aureus* , we hypothesized that GN could prevent or delay the development of a cross-kingdom biofilm on titanium.

2. Materials and methods

2.1. Sample preparation

Medical grade 4 titanium discs (Control: 12 mm diameter, 1 mm thickness, Vulcanium, USA) were polished (2500 SiC paper, EcoMet 30 Semi-Automatic Single Polisher, Buehler, Germany) and cleaned in ultrasonic bath with acetone, isopropanol, and deionized water (S30H, Elma Ultrasonic, USA; 20 min each). Graphene was produced by chemical vapour deposition and transferred onto the discs using the vacuum-assisted transfer technique (0.02 bar for 60 s) as previously described [34]. The transfer procedure was performed twice to enable a few layers graphene nanocoating on titanium discs (GN).

The coverage yields and structural integrity of ten samples were characterized by Raman spectroscopy (room temperature, with an excitation laser source of 532 nm and 0.1 mW, Raman Microscope CRM 200, Witec, Germany) for the identification of G (~1580 cm^{-1}), D (~1354 cm^{-1}) and 2D peaks (2680 cm^{-1}). After rendering the Raman mappings, ten samples were selected for surface characterization by atomic force microscope (AFM, Bruker AXS, Germany) using tapping mode with a silicon nitride tip (resonance frequency: 40-90 kHz: spring constant 0.4 N/m, 25 μm^2).

2.2. Microbial strains and culture conditions

Cross-kingdom biofilms were developed using one fungal strain (*C. albicans*, SC5314) and two *S. aureus* strains [wild type clinical ATCC 25923 and methicillin-resistant *S. aureus* (*MRSA*)] which are frequently present in infected implants and are highly resistant to antibiotics [7] .

C. albicans was sub-cultured and maintained on glucose minimal medium (GMM; Sigma-Aldrich, USA) agar plates. The plates were incubated at 30 ˚C overnight to generate fungal cells. Bacterial strains (*S. aureus* and *MRSA*) were maintained on tryptic soy (Acumedia Manufactures Inc., USA) agar plates, and incubated overnight at 37 ˚C to replicate the cells. All following liquid subcultures were derived from colonies isolated from agar plates.

To generate the cross-kingdom biofilms on titanium, fungal and bacterial strains were inoculated and incubated for 18 h in an orbital shaker incubator (80 rpm at 30 ˚C and 37 ˚C), respectively. Afterward, cells were centrifuged (4000 rpm for 5 min at 4 ˚C) and resuspended in fresh medium (1 ml) respectively. Optical density (OD) and cell suspensions were adjusted to a final concentration of 10^7 cells per/ml (OD 520 nm of 0.375–0.385 for *C. albicans* and OD 600 nm of 0.1 for *S. aureus* and *MRSA*) [35]. Thereafter, cells were spun for 10 min and washed in phosphate-buffered saline (PBS), and re-suspended in RPMI 1640 buffered with HEPES supplemented with L-glutamine (Invitrogen, USA) and 5% heat-inactivated fetal bovine serum (FBS - Hyclone™, GE Healthcare LifeSciences, USA). The discs were placed individually in 24-well plates, and 500 µl of each microorganism suspension was added to the sample to form cross-kingdom biofilms (Biofilm A: *C. albicans* + *S. aureus*; Biofilm B: *C. albicans* + *MRSA*). Finally, the plate was incubated at 37 ˚C for 24 h at 80 rpm.

2.3. Biofilm quantification and characterization

The cross-kingdom biofilms A and B grown on Control and GN were washed gently to detach the non-adherent cells by applying PBS on the side wall of the well. Thereafter, the samples were transferred to new wells and the attached biofilms were characterized by the following:

i. XTT reduction assay to evaluate the total metabolic activity of the mixed biofilm. 1 ml of XTT-menadione solution was added to the well, and incubated in the dark at 37˚C for 20 min. Finally, 200 µl of the supernatant was transferred to a new well, and the absorbance was measured at 490 nm (Multiskan GO, Thermo Scientific, USA).
ii. Crystal violet assay (CVA) to quantify total biofilm biomass. Biofilms were fixed with formalin 2% and stained with 1% (w/v) crystal violet (Sigma-Aldrich) was added into each well for 5 min. Afterward, the samples were washed three times with PBS, and 500 µl of 95% ethanol was added into each well and incubated for 15 min. Finally, 200 µl of the supernatant was transferred to a new well, and the absorbance was measured at 570 nm using a spectrophotometer. XTT or CVA assay provides total biofilm activity, not differentiating *C. albicans* from *S. aureus* in mixed-species biofilms.
iii. Colony forming unit (CFU) counting method. The biofilms were detached from the discs and dispersed upon vigorous vortexing for 3 min in PBS. A dilution series was prepared in PBS for the cell suspensions obtained from the respective biofilms. A volume of 100 µl from each dilution was plated on GMM agar (for *C. albicans*) supplemented with 10 µg/ml Chloramphenicol to prevent bacterial growth (*S. aureus* and *MRSA)* and incubated at 30 ˚C for 24 h before counting the colonies. For the quantification of *S. aureus* and *MRSA* CFUs, the 100 µl cell suspension was cultured for 24 h at 37 ˚C on TSB agar supplemented with 64 µg/ml Amphotericin B to prevent the growth of *C. albicans*.
iv. Confocal laser scanning microscopy (CLSM). The Biofilms A and B grown on Control and GN were stained for CLSM imaging in accordance with a previous protocol [36], using SYTO-9 for the bacterial cells [Invitrogen, (excitation/emission 535/617 nm)], and cal-

cofluor white [Sigma-Aldrich, (excitation/emission 365/435 nm)] for *C. albicans*. The biofilms were imaged under a confocal microscope (Olympus-Fluoview FV1000 TIRF, Japan). Four random fields were analyzed and Z sections were collected from three biological samples. Further, the biofilm biovolumes were determined (Imaris, Bitplane, Switzerland).

v. Scanning electron microscopy (SEM) The biofilms were fixed with 2% glutaraldehyde in PBS for 4 h at room temperature and dehydrated in an ascending ethanol gradient (from 25% to 100%, 5 min each). Subsequently, the samples were stored in absolute alcohol till drying to critical point with liquid CO_2, sputter-coated with gold (EM ACE600 Coater, Leica, Germany), and imaged (FEI 650 Scanning Electron Microscope, Olympus,Japan).

2.4. Hemolytic assay

The hemolytic assay aims to evaluate the hemocompatibility of biomaterials and medical devices (ISO 10993-4:2017 Biological evaluation of medical devices - Part 4: Selection of tests for interactions with blood). The use of human erythrocytes has been approved by Institutional Review Board (NUS-IRB-2022-254). Briefly, Control and GN samples (n = 3) were placed in polystyrene tubes and incubated with 500 µl of human erythrocytes (HaemoScan, Netherlands) for 1 h at 37 ˚C with shaking, and the hemolytic assay was performed as previously described [37]. Afterward, the erythrocytes were transferred to 1.5 ml tubes and centrifugated at 4,000 g for 1 min. The absorbance of the supernatant was measured at 380, 415, and 450 nm (VarioSkan LUX, Thermo Fisher Scientific, USA). The released hemoglobin concentrations were determined based on the Harboe method [38] using a hemoglobin standard curve, and the hemolysis was calculated using Eq. 1. The erythrocytes lysed in lysis buffer were used to quantify total hemoglobin (control) and tubes without the samples were the blank.

$$\text{Hemolysis } (\%) = \frac{\text{Released hemoglobin (mg/ml)}}{\text{Total hemoglobin (mg/ml)}} \times 100\% \qquad \text{(Eq. 1)}$$

2.5. Statistical analysis

All study groups had three samples and the experiments were executed in triplicates. Control was uncoated titanium discs. Mean and standard deviations were calculated for each variable. Shapiro–Wilk and Lavene's tests were performed for checking normality and homogeneity. Statistical analysis was performed using Student's t-test, one-way ANOVA with Tukey's post-hoc test. A p-value < 0.05 was considered statistically significant.

3. Results

3.1. Graphene nanocoated titanium: surface and coverage characterization

The surface of GN samples presented typical folds and bundles (arrows in Fig. 1), indicating the presence of graphene nanocoating. The Raman mappings revealed a coverage yield of 99.5%, and the 2D FWHM and I_{2D}/I_G (44 cm^{-1} and 1.2, respectively) indicate the presence of multilayer graphene on titanium. The I_D/I_G ratio of 0.09 indicates high integrity.

3.2. Cross-kingdom biofilm quantification

The cross-kingdom Biofilms A and B were grown for 24 h on the surface of Control and GN and characterized by XTT reduction and crystal violet (CVA) assays. There were significant decreases in the metabolic activity and total biofilm biomass on GN compared with the Control (Fig. 2A and B, * = $p < 0.05$).

The CFU counting was performed to quantify the number of viable cells in the biofilms. To this end, the biofilms were allowed to grow for 24 h, subsequently detached from the samples and plated on selective media for fungal or bacterial growth. The CFU counting revealed a significant reduction in the total number of viable cells on GN compared with the Control for all strains tested (Fig. 2C and D, * = $p < 0.05$).

The biofilm architectures and biovolumes were characterized by SEM and CLSM which have shown the formation of biofilms on the Control, with high adherence of bacteria to *C. albicans* with a preferred association to the hyphal elements and, to a lesser level, around the yeast cells. Conversely, biofilms on GN were disrupted and sparse with significantly less bacterial cells anchored to the reduced intermittent hyphae elements (Fig. 3 and 4). There were significant decreases in the biofilm biovolume owing to the poorly developed biofilms on GN compared with the Control (Fig. 5, * = $p < 0.05$).

Hemolysis testing was done with human erythrocytes. Both GN and Control displayed hemolytic activity under 2%, the recommended limit for hemolysis [39], and no statistical difference ($p > 0.05$) was observed (Fig. S1 in Supplementary Information).

4. Discussion

C. albicans and *S. aureus* have been co-isolated in biofilms from implanted medical devices [9]. Cross-kingdom biofilms have amplified endurance to antimicrobial agents and reduced sensitivity to host immunological defenses [8,9]. Several antimicrobial-containing strategies have been developed to avoid infection of biomaterials, but those can be ineffective against polymicrobial infections or may lead to selective microbial resistance [40,41]. Hence, developing strategies to prevent the formation or delay the growth of cross-kingdom biofilms on biomaterials is of high interest.

Cross-kingdom biofilms present higher growth dynamics and metabolic activity compared with single-species biofilms [6]. The metabolic changes during *S. aureus* and *C. albicans* co-infection modulate virulence, increase bacterial toxin production, and contribute to the remodeling from yeast to hyphae [42]. Herein, we have demonstrated the potential of graphene nanocoating in inhibiting the development of cross-kingdom biofilms on titanium surfaces. Notably, there was significantly less metabolic activity in the mixed-species biofilms grown on GN compared with the Control (Fig. 2A and B). This is remarkable, as the total biofilm activity can be a measure of the virulence of both *C. albicans* and *S. aureus* and a probable indicator of the production of hydrolytic enzymes [6]. Likewise, the CFU counting assay showed a significant decrease in the number of cells on GN (Fig. 2C and D) for all tested pathogens. This could be related to the ability of GN to exert a persistent inhibitory effect on the biofilm formation of *C. albicans* [33]. The high hydrophobicity of graphene coating is a driving force behind the lower formation of biofilms of *C. albicans,* Gram-positive and -negative bacteria on titanium [34]. Moreover, hydrophobic surfaces can potentially reduce the adherence of *S. aureus* [43]. This may be related to the fact that a superhydrophobic surface may be less prone to protein adsorption resulting in the low attachment potential of *S. aureus* [44]. Indeed, the repelling effect from GN hampers the early attachment of fungal cells [32,33]. The lower availability of fungal cells possibly decreases the amount of extracellular matrix that is important to co-aggregate *S. aureus* in polymicrobial biofilms [45]. Moreover, graphene nanocoating significantly delays the transition of *C. albicans* from yeast to hyphae form [33]. This is highly advantageous to prevent the formation of cross-kingdom biofilms since bacteria embrace and adhere to the intertwined hyphae of *C. albicans* [6,46]. Hence, the lower initial attachment of fungal cells and compromised emergence of hyphae elements on GN hinder bacterial adhesion, and the establishment and growth of robust cross-kingdom biofilm (Fig. 3 to 5).

The intricated physical and chemical interactions between bacteria and fungi favor the increase of biomass in cross-kingdom biofilm [47]. Herein, we have observed a significant 70% decrease in the biovolumes on GN, which may translate into a therapeutic advantage, as cross-kingdom biofilms display augmented tolerance toward the anti-

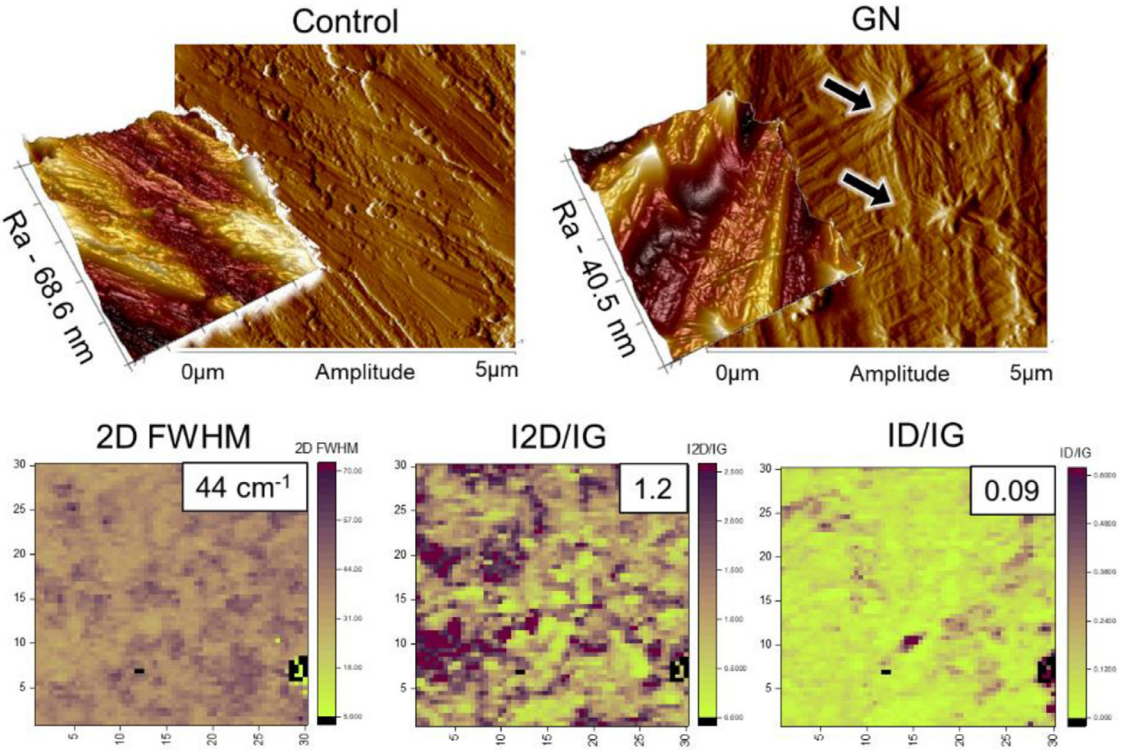

Fig. 1. Surface coverage and characteristics of graphene-coated titanium (GN). Atomic force micrographs (top) showed film folds and a lower arithmetic average of the roughness profile (R_a) for GN compared with the Control. The Raman mappings obtained from GN (below) confirmed the presence of graphene layers on titanium. The ID/IG ratio demonstrates low amount of defects (black pixels indicate the absence of graphene, mappings scale in µm).

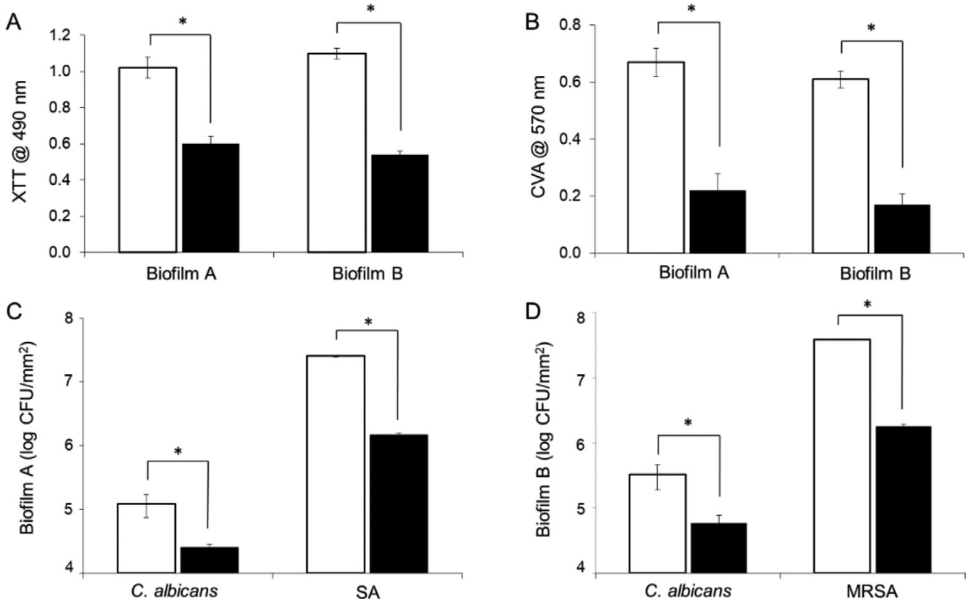

Fig. 2. Cross-kingdom biofilm formation for Biofilm A [*C. albicans* + *S. aureus* (SA)] and B (*C. albicans* + methicillin-resistant *S. aureus* (*MRSA*)] was inhibited by graphene nanocoating (GN) on the titanium surface. Both biofilms A and B showed significant decreases in the metabolic activity (XTT in A), biofilm biomass (CVA in B), and number of viable cells for each species, respectively (CFU in C and D) on GN (black bars) compared with the Control (white bars). * denotes statistical difference, $p < 0.05$.

fungals [21,22]. We also noted that biofilms on GN were thin, and scattered with lesser hyphae elements. In contrast, those formed on the Control presented the typical intertwined hyphae elements anchoring large amounts of bacterial cells (Fig. 3 to 5). This poor biofilm architecture on GN may be advantageous since dispersed biofilms are more susceptible to antibiotic treatment [48]. It is not evident if the dispersed biofilms are more sensitive to therapeutics due to the changes in biofilm morphology (leading to increased diffusion rate) or decreased biomass [48,49]. It may be possible that the biofilms with poor architectural features formed on GN are more prone to the penetration of antimicrobial agents and host immune cells. Nonetheless, this is yet to be proven.

The ability of GN to restrain cross-kingdom biofilms is of high value since almost 75% of infected implants are infected by *S. aureus* and/or *MRSA* [11]. Some of the cases can be resolved only by the surgical removal of the infected devices, which might even be life-threatening [9]. In this regard, GN offers significant advantages, as it is cytocompatible, increases bone formation *in vivo* [25,31], and can be transferred to different implant materials (e.g., titanium, stainless steel, and platinum) [50,51]. Notably, GN has not promoted hemolytic activity in human

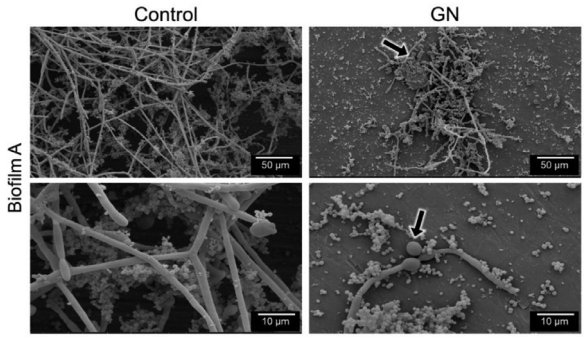

Fig. 3. Cross-kingdom biofilm A (*C. albicans* + *S. aureus*) was cultured on bare titanium (Control) or graphene nanocoating (GN) for 24 h and imaged. The SEM images revealed several hyphae elements anchoring large amounts of bacterial cells on the Control whereas the biofilm on GN was fragmented with incomplete yeast-to-hypha switching (arrows) that are essential to harbor bacterial cells (magnifications: top: 2500 X, bottom: 10000 X).

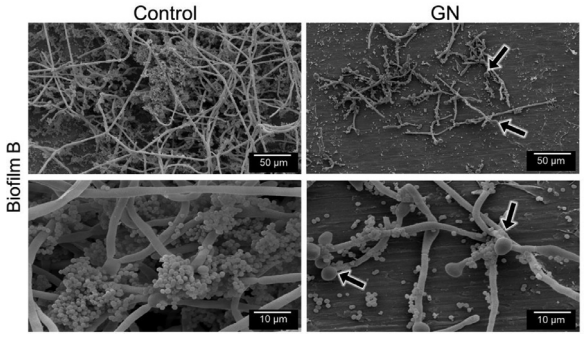

Fig. 4. Cross-kingdom biofilm B (*C. albicans* + *MRSA*) was cultured on bare titanium (Control) or graphene nanocoating (GN) for 24 h and imaged. The SEM images revealed a well-developed bundled biofilm with several bacterial cells anchored to the typical hyphae elements on the Control. Conversely, the microorganism failed to produce a robust biofilm on GN, which was sparse and contained yeast elements (arrows). (magnifications: top: 2500X, bottom: 10000X).

erythrocytes (Fig. S1, [52]). The lack of hemolytic activity is essential forblood-contacting biomaterials and devices since low hemocompatibility (high erythrocyte lysis) may result in the release of iron from red blood cells and activation of coagulation pathways [53].

It is important to note that GN did not entirely prevent biofilms formation nor eradicate them, since CVD-grown graphene films immobilized on titanium surface do not present a killing potential [31,34] which is advantageous to prevent the surge of antibiotic/fungal resistant strains. Despite the promising results, this work has some limitations. We have studied the growth of polymicrobial adhesion for 24 h and more studies are needed to characterize the potential of GN to inhibit the growth and interspecies communication of polymicrobial communities over time. However, this study provides evidence that GN has the potential to inhibit or delay the establishment of mature cross-kingdom biofilm on titanium without relying on antibiotics, biocidal or toxic substances.

5. Conclusion

Cross-kingdom biofilms of *C. albicans* with *Staphylococcus* species can cause serious problems and are related to high mortality. The strategies available mostly rely on antibiotics that can increase the risk of microbial resistance. Hence, the development of strategies that prevent the development and maturation of mixed biofilms is of high interest. Herein, the microorganisms failed to establish robust biofilms on GN as shown by the disrupted architecture, lower metabolic activity, and biovolume. Most importantly, GN was able to suppress yeast-to-hypha switching of *C. albicans* thus compromising its association with *MRSA*, which is highly virulent and very resistant to antibiotics. Hence, GN could be developed as a potential candidate to decrease the fungal and antibiotic-resistant bacterial infections on implants and implantable devices.

Funding

VR is supported by the grants from the Singapore Ministry of Education, Singapore (Academic Research Fund Tier 1, A-0002091-00-00), National Research Foundation Singapore NUS-1 NUS R&G Postdoc Fellowship Program, A-0000065-23-00) and National University Health

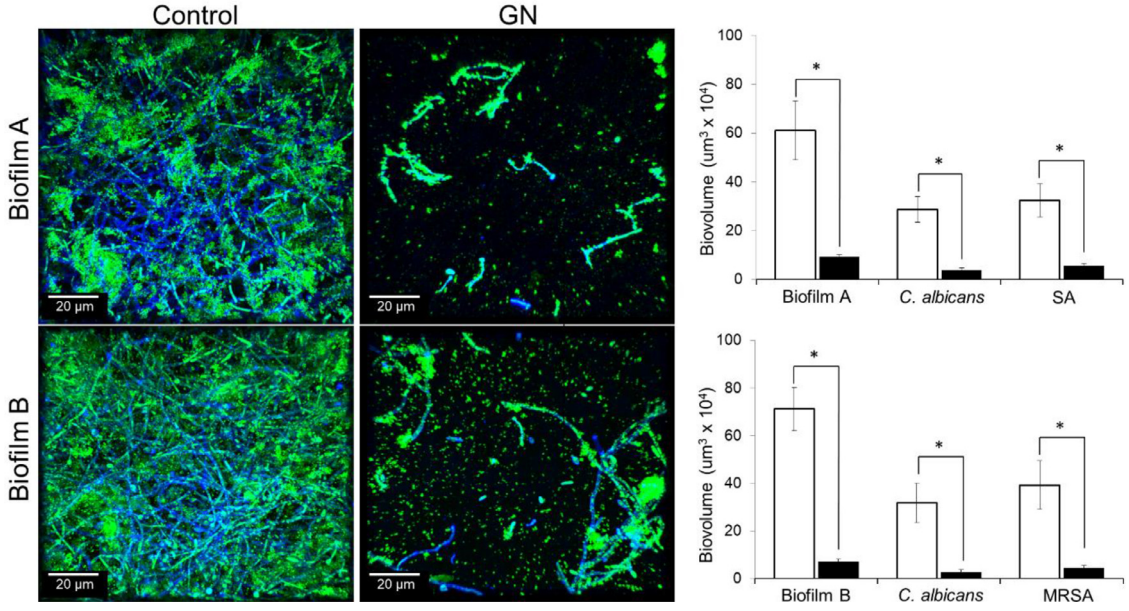

Fig. 5. Biofilm architecture and biovolume quantification. Biofilm A [*C. albicans* + *S. aureus* (SA)] and B (*C. albicans* + methicillin-resistant *S. aureus* (*MRSA*)] were stained with SYTO-9 (green, bacteria) or calcofluor (blue, *C. albicans*) and imaged with a confocal microscope. The images revealed a significant reduction of biovolume for all cross-kingdom biofilms and microbial species tested on GN compared with the Control (* = $p < 0.05$).

System, Singapore (NUHS Open Collaborative Research Grant NUHS O-CRG 2016 Oct-25). The authors acknowledge the support received from National Research Foundation Singapore.

Declaration of Competing Interest

AHCN is a shareholder of 2D Materials Pte. Ltd. All the other authors declare no Competing Financial or Non-Financial Interests.

Data Availability

Data will be made available on request.

Supplementary materials

Supplementary material associated with this article can be found, in the online version, at doi:10.1016/j.bbiosy.2022.100069.

References

[1] Chen S, Tsoi JKH, Tsang PCS, Park YJ, Song HJ, Matinlinna JP. Candida albicans aspects of binary titanium alloys for biomedical applications. Regen Biomater 2020;7:213–20. doi:10.1093/rb/rbz052.
[2] Osman RB, Swain MV. A Critical Review of Dental Implant Materials with an Emphasis on Titanium versus Zirconia. Materials (Basel) 2015;8:932–58. doi:10.3390/ma8030932.
[3] Terawaki H, Nakano H, Ogura M, Kadomura M, Hosoya T, Nakayama M. Unroofing Surgery with en Bloc Resection of the Skin and Tissues Around the Peripheral Cuff. Peritoneal Dialysis International: Journal of the International Society for Peritoneal Dialysis 2013;33:573–6. doi:10.3747/pdi.2012.00262.
[4] Bracke F. Complications and lead extraction in cardiac pacing and defibrillation. Neth Heart J 2008;16:S28–31.
[5] Peters BM, Jabra-Rizk MA, O'May GA, Costerton JW, Shirtliff ME. Polymicrobial interactions: impact on pathogenesis and human disease. Clin Microbiol Rev 2012;25:193–213. doi:10.1128/CMR.00013-11.
[6] Zago CE, Silva S, Sanita PV, Barbugli PA, Dias CM, Lordello VB, et al. Dynamics of biofilm formation and the interaction between Candida albicans and methicillin-susceptible (MSSA) and -resistant Staphylococcus aureus (MRSA). PLoS One 2015;10:e0123206. doi:10.1371/journal.pone.0123206.
[7] Kong EF, Tsui C, Kucharíková S, Andes D, Van Dijck P, Jabra-Rizk MA, et al. Commensal Protection of Staphylococcus aureus against Antimicrobials by Candida albicans Biofilm Matrix. mBio 2016;7. doi:10.1128/mBio.01365-16.
[8] Seneviratne CJ, Jin L, Samaranayake LP. Biofilm lifestyle of Candida: a mini review. Oral Dis 2008;14:582–90. doi:10.1111/j.1601-0825.2007.01424.x.
[9] Kucharikova S, Gerits E, De Brucker K, Braem A, Ceh K, Majdic G, et al. Covalent immobilization of antimicrobial agents on titanium prevents Staphylococcus aureus and Candida albicans colonization and biofilm formation. J Antimicrob Chemother 2016;71:936–45. doi:10.1093/jac/dkv437.
[10] Beck-Sague C, Jarvis WR. Secular trends in the epidemiology of nosocomial fungal infections in the United States, 1980-1990. National Nosocomial Infections Surveillance System. J Infect Dis 1993;167:1247–51. doi:10.1093/infdis/167.5.1247.
[11] Oliveira WF, Silva PMS, Silva RCS, Silva GMM, Machado G, Coelho L, et al. Staphylococcus aureus and Staphylococcus epidermidis infections on implants. J Hosp Infect 2018;98:111–17. doi:10.1016/j.jhin.2017.11.008.
[12] Teterycz D, Ferry T, Lew D, Stern R, Assal M, Hoffmeyer P, et al. Outcome of orthopedic implant infections due to different staphylococci. Int J Infect Dis 2010;14:e913–e9e8. doi:10.1016/j.ijid.2010.05.014.
[13] Rehm SJ, Tice A. Staphylococcus aureus: methicillin-susceptible S. aureus to methicillin-resistant S. aureus and vancomycin-resistant S. aureus. Clin Infect Dis 2010;51(Suppl 2):S176–82. doi:10.1086/653518.
[14] Carlson E. Effect of strain of Staphylococcus aureus on synergism with Candida albicans resulting in mouse mortality and morbidity. Infect Immun 1983;42:285–92.
[15] Carlson EC. Synergism of Candida albicans and delta toxin producing Staphylococcus aureus on mouse mortality and morbidity: protection by indomethacin. Zentralbl Bakteriol Mikrobiol Hyg A 1988;269:377–86. doi:10.1016/s0176-6724(88)80181-0.
[16] Baena-Monroy T, Moreno-Maldonado V, Franco-Martinez F, Aldape-Barrios B, Quindos G, Sanchez-Vargas LO. Candida albicans, Staphylococcus aureus and Streptococcus mutans colonization in patients wearing dental prosthesis. Med Oral Patol Oral Cir Bucal 2005;10(Suppl 1):E27–39.
[17] Crnich CJ, Maki DG. The Promise of Novel Technology for the Prevention of Intravascular Device–Related Bloodstream Infection. I. Pathogenesis and Short-Term Devices. Clin Infect Dis 2002;34:1232–42. doi:10.1086/339863.
[18] Nart J, Pons R, Valles C, Esmatges A, Sanz-Martín I, Monje A. Non-surgical therapeutic outcomes of peri-implantitis: 12-month results. Clin Oral Investig 2019;24:675–82. doi:10.1007/s00784-019-02943-8.
[19] Alhag M, Renvert S, Polyzois I, Claffey N. Re-osseointegration on rough implant surfaces previously coated with bacterial biofilm: an experimental study in the dog. Clin Oral Implants Res 2008;19:182–7. doi:10.1111/j.1600-0501.2007.01429.x.
[20] Harriott MM, Noverr MC. Ability of Candida albicans mutants to induce Staphylococcus aureus vancomycin resistance during polymicrobial biofilm formation. Antimicrob Agents Chemother 2010;54:3746–55. doi:10.1128/AAC.00573-10.
[21] Adam B, Baillie GS, Douglas LJ. Mixed species biofilms of Candida albicans and Staphylococcus epidermidis. J Med Microbiol 2002;51:344–9. doi:10.1099/0022-1317-51-4-344.
[22] Kean R, Rajendran R, Haggarty J, Townsend EM, Short B, Burgess KE, et al. Candida albicans Mycofilms Support Staphylococcus aureus Colonization and Enhances Miconazole Resistance in Dual-Species Interactions. Front Microbiol 2017;8:258. doi:10.3389/fmicb.2017.00258.
[23] Verdugo F, Laksmana T, Uribarri A. Systemic antibiotics and the risk of superinfection in peri-implantitis. Arch Oral Biol 2016;64:39–50. doi:10.1016/j.archoralbio.2015.12.007.
[24] Brogden K, Guthmiller J, Taylor C. Human polymicrobial infections. Lancet North Am Ed 2005;365:253–5. doi:10.1016/s0140-6736(05)70155-0.
[25] Dubey N, Morin JLP, Luong-Van EK, Agarwalla SV, Silikas N, Castro Neto AH, et al. Osteogenic potential of graphene coated titanium is independent of transfer technique. Materialia 2020;9. doi:10.1016/j.mtla.2020.100604.
[26] Dubey KE N, Decroix FED, Morin JLP, Castro Neto A, Seneviratne CJ, Rosa V. Graphene onto medical grade titanium: an atom-thick multimodal coating that promotes osteoblast maturation and inhibits biofilm formation from distinct species. Nanotoxicology 2018;12:274–89. doi:10.1080/17435390.2018.1434911.
[27] Rosa V, Malhotra R, Agarwalla SV, Morin JLP, Luong-Van EK, Han YM, et al. Graphene Nanocoating: High Quality and Stability upon Several Stressors. J Dent Res 2021;100:1169–77. doi:10.1177/00220345211024526.
[28] Xie H, et al. Two and three-dimensional graphene substrates to magnify osteogenic differentiation of periodontal ligament stem cells. Carbon 2015;93:266–75. doi:10.1016/j.carbon.2015.05.071.
[29] Xie H, Cao T, Franco-Obregón A, Rosa V. Graphene-Induced Osteogenic Differentiation Is Mediated by the Integrin/FAK Axis. Int J Mol Sci 2019;20. doi:10.3390/ijms20030574.
[30] Kalbacova M, Broz A, Kong J, Kalbac M. Graphene substrates promote adherence of human osteoblasts and mesenchymal stromal cells. Carbon 2010;48:4323–9. doi:10.1016/j.carbon.2010.07.045.
[31] Dubey N, Ellepola K, Decroix FED, Morin JLP, Castro Neto AH, Seneviratne CJ, et al. Graphene onto medical grade titanium: an atom-thick multimodal coating that promotes osteoblast maturation and inhibits biofilm formation from distinct species. Nanotoxicology 2018;12:274–89. doi:10.1080/17435390.2018.1434911.
[32] Agarwalla SV, Ellepola K, Costa MCF, Fechine GJM, Morin JLP, Castro Neto AH, et al. Hydrophobicity of graphene as a driving force for inhibiting biofilm formation of pathogenic bacteria and fungi. Dent Mater 2019;35:403–13. doi:10.1016/j.dental.2018.09.016.
[33] Agarwalla SV, Ellepola K, Silikas N, Castro Neto AH, Seneviratne CJ, Rosa V. Persistent inhibition of Candida albicans biofilm and hyphae growth on titanium by graphene nanocoating. Dent Mater 2021;37:370–7. doi:10.1016/j.dental.2020.11.028.
[34] Agarwalla SV, Ellepola K, Costa M, Fechine GJM, Morin JLP, Castro Neto AH, et al. Hydrophobicity of graphene as a driving force for inhibiting biofilm formation of pathogenic bacteria and fungi. Dent Mater 2019;35:403–13. doi:10.1016/j.dental.2018.09.016.
[35] Peters BM, Jabra-Rizk MA, Scheper MA, Leid JG, Costerton JW. Shirtliff ME. Microbial interactions and differential protein expression in Staphylococcus aureus -Candida albicans dual-species biofilms. FEMS Immunol Med Microbiol 2010;59:493–503. doi:10.1111/j.1574-695X.2010.00710.x.
[36] Ellepola KL, Cao Y, Koo T, Seneviratne H, J C. Bacterial GtfB Augments Candida albicans Accumulation in Cross-Kingdom Biofilms. J Dent Res 2017:22034517714414. doi:10.1177/0022034517714414.
[37] Zhou C, Li Z, Zhu Z, Chia GWN, Mikhailovsky A, Vazquez RJ, et al. Conjugated Oligoelectrolytes for Long-Term Tumor Tracking with Incremental NIR-II Emission. Adv Mater 2022;34:e2201989. doi:10.1002/adma.202201989.
[38] Fairbanks VF, Ziesmer SC, O'Brien PC. Methods for measuring plasma hemoglobin in micromolar concentration compared. Clin Chem 1992;38:132–40.
[39] Wersig T, Krombholz R, Janich C, Meister A, Kressler J, Mader K. Indomethacin functionalised poly(glycerol adipate) nanospheres as promising candidates for modified drug release. Eur J Pharm Sci 2018;123:350–61. doi:10.1016/j.ejps.2018.07.053.
[40] Hoffman LR, D'Argenio DA, MacCoss MJ, Zhang Z, Jones RA, Miller SI. Aminoglycoside antibiotics induce bacterial biofilm formation. Nature 2005;436:1171–5. doi:10.1038/nature03912.
[41] Kozlovsky A, Artzi Z, Moses O, Kamin-Belsky N, Greenstein RB. Interaction of chlorhexidine with smooth and rough types of titanium surfaces. J Periodontol 2006;77:1194–200. doi:10.1902/jop.2006.050401.
[42] Eichelberger KR, Cassat JE. Metabolic Adaptations During Staphylococcus aureus and Candida albicans Co-Infection. Front Immunol 2021;12. doi:10.3389/fimmu.2021.797550.
[43] Zhang X WL, Levänen E. Superhydrophobic surfaces for the reduction of bacterial adhesion. RSC Adv 2013;3:12003–20.
[44] Stallard CP, McDonnell KA, Onayemi OD, O'Gara JP, Dowling DP. Evaluation of protein adsorption on atmospheric plasma deposited coatings exhibiting superhydrophilic to superhydrophobic properties. Biointerphases 2012;7:31. doi:10.1007/s13758-012-0031-0.
[45] Harriott MM, Noverr MC. Candida albicans and Staphylococcus aureus form polymicrobial biofilms: effects on antimicrobial resistance. Antimicrob Agents Chemother 2009;53:3914–22. doi:10.1128/AAC.00657-09.
[46] Tarifa MC, Lozano JE, Brugnoni LI. Dual-species relations between Candida tropicalis isolated from apple juice ultrafiltration membranes, with Escherichia coli O157:H7 and Salmonella sp. J Appl Microbiol 2015;118:431–42. doi:10.1111/jam.12710.

[47] Bamford CV, d'Mello A, Nobbs AH, Dutton LC, Vickerman MM, Jenkinson HF. Streptococcus gordonii modulates Candida albicans biofilm formation through intergeneric communication. Infect Immun 2009;77:3696–704. doi:10.1128/IAI.00438-09.
[48] Wille J, Coenye T. Biofilm dispersion: The key to biofilm eradication or opening Pandora's box? Biofilm 2020;2. doi:10.1016/j.bioflm.2020.100027.
[49] Barraud N, Hassett DJ, Hwang S-H, Rice SA, Kjelleberg S, Webb JS. Involvement of Nitric Oxide in Biofilm Dispersal of Pseudomonas aeruginosa. J Bacteriol 2006;188:7344–53. doi:10.1128/jb.00779-06.
[50] Rodriguez CLC, Kessler F, Dubey N, Rosa V, Fechine GJM. CVD graphene transfer procedure to the surface of stainless steel for stem cell proliferation. Surf Coat Technol 2017;311:10–18. doi:10.1016/j.surfcoat.2016.12.111.
[51] Morin JLP, Dubey N, Decroix FED, Luong-Van EK, Castro Neto AH, Rosa V. Graphene transfer to 3-dimensional surfaces: a vacuum-assisted dry transfer method. 2D Mater 2017;4. doi:10.1088/2053-1583/aa6530.
[52] American Society for Testing and Materials ASTM F. 756-00. Standard practice for assessment of hemolytic properties of materials; 2000.
[53] Liu X, Yuan L, Li D, Tang Z, Wang Y, Chen G, et al. Blood compatible materials: state of the art. J Mater Chem B 2014;2:5718–38. doi:10.1039/c4tb00881b.